

RESEARCH ARTICLE

Delayed access to conscious processing in multiple sclerosis: Reduced cortical activation and impaired structural connectivity

Arzu C. Has Silemek¹  | Jean-Philippe Ranjeva^{2,3}  | Bertrand Audoin^{2,3} |
 Christoph Heesen^{1,4} | Stefan M. Gold^{1,5} | Simone Kühn^{6,7}  |
 Martin Weygandt^{8,9}  | Jan-Patrick Stellmann^{1,2,3,4} 

¹Institut für Neuroimmunologie und Multiple Sklerose (INIMS), Universitätsklinikum Hamburg-Eppendorf (UKE), Hamburg, Germany

²Aix-Marseille University, CNRS, CRMBM, Marseille Cedex, France

³APHM, Hopital de la Timone, CEMEREM, Marseille, France

⁴Klinik und Poliklinik für Neurologie, Universitätsklinikum Hamburg-Eppendorf, Hamburg, Germany

⁵Charité - Universitätsmedizin Berlin, Freie Universität Berlin, Humboldt Universität zu Berlin, and Berlin Institute of Health (BIH), Klinik für Psychiatrie & Psychotherapie und Medizinische Klinik m.S. Psychosomatik, Campus Benjamin Franklin (CBF), Berlin, Germany

⁶Clinic for Psychiatry and Psychotherapy, University Medical Center Hamburg-Eppendorf, Hamburg, Germany

⁷Lise Meitner Group for Environmental Neuroscience, Max Planck Institute for Human Development, Berlin, Germany

⁸Max Delbrück Center for Molecular Medicine and Charité - Universitätsmedizin Berlin, corporate member of Freie Universität Berlin, Humboldt-Universität zu Berlin, and Berlin Institute of Health, Experimental and Clinical Research Center, Berlin, Germany

⁹Charité - Universitätsmedizin Berlin, corporate member of Freie Universität Berlin, Humboldt-Universität zu Berlin, and Berlin Institute of Health, NeuroCure Clinical Research Center, Berlin, Germany

Correspondence

Arzu C. Has Silemek, Institut für Neuroimmunologie und Multiple Sklerose,

Abstract

Although multiple sclerosis (MS) is frequently accompanied by visuo-cognitive impairment, especially functional brain mechanisms underlying this impairment are still not well understood. Consequently, we used a functional MRI (fMRI) backward masking task to study visual information processing stratifying unconscious and conscious in MS. Specifically, 30 persons with MS (pwMS) and 34 healthy controls (HC) were shown target stimuli followed by a mask presented 8–150 ms later and had to compare the target to a reference stimulus. Retinal integrity (via optical coherence tomography), optic tract integrity (visual evoked potential; VEP) and whole brain structural connectivity (probabilistic tractography) were assessed as complementary structural brain integrity markers. On a psychophysical level, pwMS reached conscious access later than HC (50 vs. 16 ms, $p < .001$). The delay increased with disease duration ($p < .001$, $\beta = .37$) and disability ($p < .001$, $\beta = .24$), but did not correlate with conscious information processing speed (Symbol digit modality test, $\beta = .07$, $p = .817$). No association was found for VEP and retinal integrity markers. Moreover, pwMS were characterized by decreased brain activation during unconscious processing compared with HC. No group differences were found during conscious processing. Finally, a complementary structural brain integrity analysis showed that a reduced fractional anisotropy in corpus callosum and an impaired connection between right insula and primary visual areas was related to delayed conscious access in pwMS. Our study revealed slowed conscious access to visual stimulus material in MS and a complex pattern of functional and structural alterations coupled to unconscious processing of/delayed conscious access to visual stimulus material in MS.

KEYWORDS

(un)consciousness, anterior visual system, functional magnetic resonance imaging, multiple sclerosis, optical coherence tomography, structural connectivity, visual backward masking paradigm

This is an open access article under the terms of the Creative Commons Attribution-NonCommercial-NoDerivs License, which permits use and distribution in any medium, provided the original work is properly cited, the use is non-commercial and no modifications or adaptations are made.

© 2021 The Authors. *Human Brain Mapping* published by Wiley Periodicals LLC.

Universitätsklinikum Hamburg-Eppendorf,
Germany, Martinistrasse 52, 20246 Hamburg,
Germany.
Email: a.has@uke.de

1 | INTRODUCTION

Multiple sclerosis (MS) is a chronic inflammatory and neurodegenerative disease of the central nervous system (DeLuca, Chiaravalloti, & Sandroff, 2020) and people with MS (pwMS) suffer from accumulating impairment in multiple functional systems (Pinto et al., 2020). From a patients' perspective cognition and vision are two of the three most valuable bodily functions besides mobility (Heesen et al., 2018). While 40–70% of pwMS have cognitive impairments in information processing speed, episodic memory, and executive function (Julian, 2011; Sumowski et al., 2018), more than 50% of pwMS are also affected by visual deficits (Balcer, Miller, Reingold, & Cohen, 2015). Retinal integrity and visual acuity are correlated with cognitive performance like information processing speed and memory (Bruce, Bruce, & Arnett, 2007; Jakimovski et al., 2021; Nguyen et al., 2018; Wieder et al., 2013). Processing of visual information might be compromised anywhere between the retina and higher-level brain areas and effect thus cognitive performance (van Gaal, de Lange, & Cohen, 2012).

Cognition in general needs both conscious (Ansorge, Kunde, & Kiefer, 2014) and unconscious information processing (Horga & Maia, 2012). Specifically, cognitive functions including working memory (Soto, Mäntylä, & Silvanto, 2011), inhibitory control (Van Gaal, Ridderinkhof, Scholte, & Lamme, 2010), task selection (Lau & Passingham, 2007) and decision-making (Custers & Aarts, 2010; Pessiglione et al., 2008) are known to be effected by unconscious processing of visual information. For visual information, the initial processing between the retina and the primary visual cortical areas can be considered as unconscious (Leopold, 2012). However, beyond the primary visual system, spatially segregated brain pathways of unconscious and conscious processing have been identified. In this context, the so called two stream theory describes the basic topology of the information flow beyond primary visual areas (Milner & Goodale, 2008; Narain, 2005). The dorsal stream (“where,” parietal lobe) is known to be related with unconscious visual processing while the ventral stream (“what,” temporal lobe) belongs to the conscious processing (Rossetti, Pisella, & McIntosh, 2017). Conceptually, all information are initially processed unconsciously and impaired structural connection might result in higher rates of stimuli that fail to reach consciousness but might be important for high level cognitive functions (Dijksterhuis & Nordgren, 2006; Marchetti, 2018). Therefore, dealing with the access consciousness could be important for the cognitive impairment in MS. However, it is yet unclear in how far the transition from unconscious processing to conscious processing is altered in MS and how and where it is associated with impaired visual system.

Backward masking is an established technique to study visuo-cognitive information processing (Breitmeyer & Ogmen, 2000; Stein &

Sterzer, 2014) that allows to distinguish and evaluate performance for unconscious and conscious processing as well as to estimate the transition from one to the other (Breitmeyer & Ogmen, 2010). Brain regions triggered by such a task can be identified by functional magnetic resonance imaging (fMRI). So far, occipital inferior parietal, prefrontal, and cingulate cortex have been associated with visual backward masking using task based fMRI in healthy controls (HC) (Dehaene et al., 2001; Diaz & McCarthy, 2007; Green et al., 2005; Kleinschmidt, Büchel, Hutton, Friston, & Frackowiak, 2002; Kranczioch, Debener, Schwarzbach, Goebel, & Engel, 2005; Lau & Passingham, 2006; Sterzer, Haynes, & Rees, 2008; Watanabe et al., 2011) as well as in schizophrenia patients (Berkovitch, Del Cul, Maheu, & Dehaene, 2018; Green et al., 2009; Lee et al., 2014) and in a case report of epilepsy patient (Gaillard et al., 2006). However, it is still not known whether there is a similar or specific activation pattern in pwMS.

In this study, we aimed to explore the alterations within the visual processing pathways and their relationship with conscious and unconscious processing during a backward-masking task in MS. To follow this aim we combined clinical assessments, optical coherence tomography (OCT), visual evoked potential (VEP), structural MRI, and DTI with the fMRI task. We hypothesized that MS patients show impaired performance during the task and a longer access time to conscious processing compared with healthy controls. Moreover, we assumed that such findings correlate with altered functional cortical activation and structural alterations in the visual pathways.

2 | METHODS

2.1 | Participants, clinical assessments, and data acquisition

We recruited pwMS and HC through the MS day clinic of the Institute of Neuroimmunology and Multiple Sclerosis (INIMS) between January 2019 and January 2020. Participants were not related. All participants gave written informed consent prior to any testing under this protocol. We obtained ethical approval from the local ethic committee of Hamburg Chamber of Physicians (Registration Number PV5557). For the MS group, the following inclusion criteria were applied: (a) MS based on the revised McDonald criteria 2010 (Polman et al., 2011) (b) EDSS score; 0–6.0 for Relapsing–remitting MS and 3.0–6.0 for the progressive MS cohort based on the Lorscheider et al. (Lorscheider et al., 2016); (c) no relapse in the last 12 month. The following inclusion criteria were applied for both HC and pwMS: (d) no other major neurological or psychiatric disorder (such as depression or schizophrenia); (e) naïve to psychoactive drugs such as antidepressants; (f) age between 18 and 65 years. HC and pwMS were excluded based on the

following criteria: cataract and other ophthalmological diseases (such as uveitis and glaucoma), neuromyelitis optical spectrum disease, astigmatism higher than 3 dpt, hyperopia higher than 5 dpt and myopia lower than -7 dpt.

All participants underwent a clinical assessment including outcomes for disability, cognitive performance and vision. Moreover, we performed an OCT to determine retinal integrity, VEP and a MRI session including the backward masking fMRI-task, conventional T1- and T2-structural imaging and DTI. All assessments were performed within the same day.

2.1.1 | Clinical assessments

Disability of pwMS was assessed by the expanded disability status scale (EDSS) (Kurtzke, 1983). The symbol digit modalities test (SDMT) (Smith, 1982) was used as an indicator of the overall cognitive function although it measures mainly information processing speed (Benedict et al., 2017). For descriptive purposes, we report SDMT values as *SD* from available norm data adjusted for sex, age and education (Köhler et al., 2017). 9-Hole Peg Test (NHPT) (Backman et al., 1992; Chan, 2000) and the Timed-25 food walk (T25FW) were used in the neurological assessment. All participants performed a visual system assessment including OCT, VEP, high contrast visual acuity (HCVA) at a distance of 5 m (Snellen), low contrast visual acuity (LCVA, Sloan charts at 2.5%) and the area under the log contrast sensitivity function (AULCSF) assessed with the quantitative contrast sensitive function (qCSF) test which is a computerized test which uses a Bayesian adaptive method to assess the full CSF (Stellmann, Young, Pöttgen, Dorr, & Heesen, 2015). The complete contrast sensitivity function with a combination of different contrasts were detected by a device qualified by three bandpass-filtered Sloan letters in each of 25 trials with three letters on a 46-in. computer screen at a 5 m viewing distance.

2.1.2 | Optical coherence tomography

OCT measurements were acquired by Heidelberg-Spectralis SD-OCT System by experienced operators. Macular volume and individual retinal layer (thickness) assessments comprised $30^\circ \times 25^\circ$ OCT volume scan protocol (61 B-scans; ART = 13 frames) centered on the fovea and a ring scan centered on the optic nerve head. All scans were checked for OSCAR-IB quality criteria. Then, retinal layers were segmented semi-automatically. Retinal nerve fiber layer thickness (RNFL) was calculated on a 3 mm ring. Total macular volume and ganglion cell/inner plexiform layer (GCIPL) volume were extracted as 3 mm cylinder around the fovea centralis.

2.1.3 | VEP

VEP of each patient was recorded with a Nihon Kohden Neuropack System (Nihon Kohden Europe GmbH, Rosbach, Deutschland). The

examination consisted of a fixed protocol for all subjects and took place in a dark room. Display to eye distance was 120 cm and we used full-field monocular stimulation by pattern reversal black on white checkerboards. Two electrodes, fc (on top of the head, frontal central) and oc (occipital central, at the back of the head) were positioned. Electrical grounding was fixed on the lower left hand. Potentials were measured at a frequency of 1 Hz and 5 μ A and P100 latencies which shows as peak followed by a deep drop of the curve were calculated. The examination was done twice for each eye, where one examination consisted of at least 60 averaged measurements. During the examination, participants covered the unexamined eye by holding their hand or wearing an eyepatch and were seated in a comfortable chair. Wearing a glass or contact-lens, and so forth during the examination was mandatory if it is needed.

2.1.4 | MRI data acquisition

All participants underwent a 3 T MRI equipped with 32-channel head coil (Prisma, Siemens Medical Systems, Erlangen, Germany). The same MRI protocol was applied to all participants and included DTI, the task-based fMRI and conventional structural MR imaging. Conventional MRI involved 3D T1-weighted (W) magnetization-prepared rapid acquisition with gradient echo (MPRAGE) for calculation of high-resolution volume/cortical thickness and T2-weighted and Flair sequences for lesion masking. Please find the parameters of each MRI sequence in Supporting Information (SI) *MRI data acquisition*.

2.2 | Experimental design of task-based fMRI

We used a modified version of the visual backward masking paradigm (Reuter et al., 2009) adapted to a task-based fMRI experiment. The task is considered to be a valuable tool to study visual information processing (including visual awareness and attention) throughout the entire visual system up to high level cognitive processes. The two major mechanisms of the paradigm are probably the erasure or the interrupt of the stimulus processing by the mask. The task has been recognized as providing reliable experimental estimates about the transition from nonconscious to conscious perception (Breitmeyer & Ogmen, 2000). The fMRI stimulus for the masking experiment was created by Psychophysics Toolbox Version-3 in MATLAB (<http://psychtoolbox.org/>). In the masking experiment, first, a target number (1, 4, 6, or 9) (color: black, Arabic number, font: courier new, size: 20, background-color: white, that is, high contrast) was presented during 16 ms in one of four locations relative to 1.4° visual angle to the fixation cross. Then, after one of randomly presented eight possible stimulus onset asynchronies (SOA): 8, 16, 33, 50, 66, 83, 100, 150 ms, the mask including another number (1, 4, 6, or 9) and three letters (E, M, E) was placed around the target number without touching it for 250 ms at 1° from the fixation cross (Figure 1). SOAs were presented in a block-wise fashion (eight blocks for eight SOAs). Since previous studies detected strong correlations between subjective and objective

measures for pwMS and HC (Reuter et al., 2007, 2009), we obtained only objective measures. Participants were asked to compare the target number with five and responses were collected with two buttons (right hand: target >5, left hand: target <5). Each trial lasted for 2 s and each block for each SOA involved 40 trials (Figure 1). After each block, a white screen with a fixation cross was presented as a resting block for 30 s. This design was presented via an LCD screen in the scanner room which had resolution: 1920 x 1,200 (60 Hz), 24" screen, 52 cm wide and 115 cm from the participant's eyes to the screen.

2.3 | Behavioral data

We computed the accuracy (% of correct answers) as the primary performance outcome for each SOA. Missing responses within the 2 s trial duration were treated as wrong answers. Accuracy (objective performance) was treated as a nonlinear function of the SOA and the point of the fastest increase in accuracy, corresponding to the inflection point is the access threshold to conscious processing, characterizing the transition between unconscious (i.e., subliminal and/or preconscious processing in the existence of the lack of awareness) and conscious processing (Del Cul, Baillet, & Dehaene, 2007). To obtain access threshold to conscious processing (inflection point) for both each person and each group, we used nonlinear regression to estimate the objective performance as a function of SOA using Taylor regression estimator which is available in the RootsExtremalInflections package of R (Christopoulos, 2014) and can

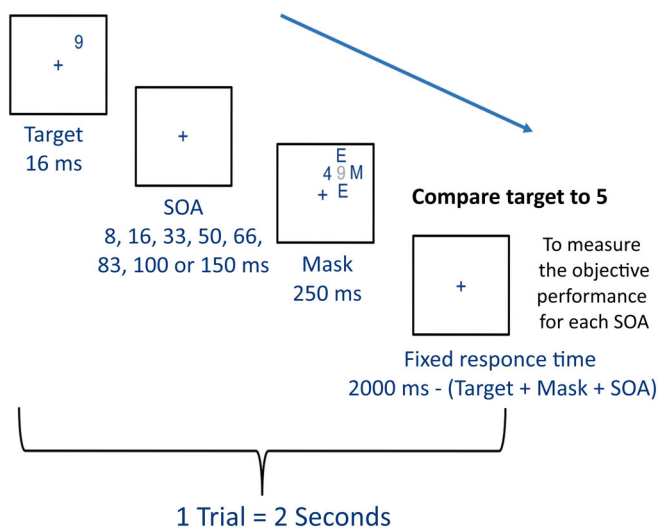


FIGURE 1 Design of the fMRI experiment. The target was presented in one of four positions for 16 ms (1.4° visual angle to the fixation cross). The mask was presented as three letters (E, M, and E) and another number (1, 4, 6, or 9) during 250 ms at 1° from the fixation cross. The mask enclosure was placed around the target number without touching it. The subjects were asked to press the right button if the target number was greater than 5 and the left button if it was less than 5. The illustrated design for a single trial was repeated 40 times for each stimulus onset asynchrony (SOA) and followed by a resting block of 30 s

work for discrete and noisy values. In this method, Taylor polynomial of a smooth function f around a point ρ is used:

$$f(x) = a_0 + a_1(x-\rho) + a_2(x-\rho)^2 + a_3(x-\rho)^3 + \dots + a_n(x-\rho)^n$$

At the minimum absolute value of the coefficient a_2 , the corresponding point ρ is the estimator of *inflection point*.

Reaction times were also recorded.

2.4 | Analysis of task-based fMRI

Preprocessing of the fMRI data were done as described in Bowring et al., (Bowring, Maumet, & Nichols, 2019) using SPM12 (Ashburner et al., 2013). Briefly, to adjust for head motion, geometric distortions and physiological effects such as random drifts, breathing, and heartbeats, we applied slice timing and realignment to the fMRI data. Following the spatial normalization to the MNI space, the normalized data was smoothed by 8 mm full width at half maximum (FWHM) Gaussian kernel. The preprocessed data of each participant were then entered into the first level analysis where the data were modeled for each of the following three experimental conditions: conscious, unconscious and neutral. We used the groups' average access threshold to conscious processing to define unconscious SOAs (SOA < = inflection point) and conscious SOAs (SOA > inflection point) blocks. We extracted five different contrasts; conscious, unconscious, conscious versus neutral and unconscious versus neutral and whole SOAs versus neutral for each subject. Before the group comparison, whole SOAs versus neutral contrast of each subject was entered into a one sample t test to extract the fixed effect in each group. Then, the group differences (pwMS vs. HC) of each contrast were calculated. All results were corrected for the multiple comparison as mentioned in the Statistics session at cluster and at voxel level.

2.5 | Processing of structural imaging data

Processing of structural MR imaging data included the following steps: First, to avoid segmentation errors, we performed lesion filling on T1W. T2W images was used to identify and outline manually the lesions. For this aim; T1W images were registered to MNI template and then to T2W for each subject using functional imaging software library (FSL, version 5.0, www. fmrib.ox.ac.uk). Then, lesion maps [T1-hypo and T2-hyper] were extracted semi-automatically by Analyze 11.0 software (AnalyzeDirect, www.analyzedirect.com). Following the masking, lesion-filling procedure was performed using FSL (FSL, version 5.0, www. fmrib.ox.ac.uk).

After lesion-filling, an automated procedure was performed on T1 to assess the volume and cortical thickness for each subject using Freesurfer (Fischl et al., 2002). For the successful segmentation of the whole brain, the automated algorithm included removal of nonbrain tissue (skull, eyeballs and skin). For obtaining the regional measures of cortical volumes, cortical surface reconstruction methods were involved. Following the removal of white matter residual which is

involved in “*autorecon*” processing steps of Freesurfer (<https://surfer.nmr.mgh.harvard.edu/fswiki/recon-all>), each subject was registered to Destrieux atlas using spherical registration. White matter and gray matter volume of each subject was divided by total intracranial volume of each subject to normalize the calculated parenchymal fraction. In addition, we manually corrected the brain masks and gray/white matter segmentations for each subject. Finally, gray-matter parcellation of 80 regions (total: 160) for each hemisphere was specified based on the Destrieux atlas (2009) (Destrieux, Fischl, Dale, & Halgren, 2010) to perform the structural connectivity analysis. The FreeSurfer fsaverage subject was used to detect each node's location.

We then compared cortical thickness between pwMS and controls and extracted the correlation between cortical thickness and the time to access consciousness using general linear model (GLM) controlling for age and sex using Freesurfer's Qdec (www.surfer.nmr.mgh.harvard.edu) (See Supporting Information *Cortical thickness*).

We calculated the structural connectivity based on the probabilistic tractography. Please find the detailed information of the processing in the section of “*Structural connectivity*” at Supporting Information. Briefly, probabilistic tractography was performed using MRTRIX3 (Tournier et al., 2019) as described in Besson et al. (2014) in a recent paper from our group (Has Silemek et al., 2020). FSL software (Behrens, Berg, Jbabdi, Rushworth, & Woolrich, 2007) was used to perform the preprocessing of the DTI data and then to extract the DTI fitting. Strength as a measure of structural connectivity was calculated as the sum of weighted connections within and between each node for each subject. To extract the structural connectivity matrices, mean FA between every pair of gray matter regions i and j that had at least one fiber with a minimum length threshold of 20 mm exceed a threshold of 0.7.

2.5.1 | Network based statistics

To perform statistical correlations and group comparison analysis of structural connections that we extracted in the Section 2.5, we used the networks based statistics (NBS) (Zalesky, Fornito, & Bullmore, 2010) toolbox implemented in MATLAB R2016 as describe in McColgan et al. (McColgan et al., 2017). We predefined a stepwise selection approach to identify regions (nodes) and connections (edges) that are associated with the time to access consciousness. First, we extracted subnetworks including only those nodes and edges that showed a significant correlation with the inflection point—either in patients or controls. Next, we determined which part of these networks differed significantly between patients and controls. In NBS, first, a t statistic is calculated for each individual edge of the connectivity network. A set of suprathreshold connections was formed by a primary threshold of $p < .05$ (uncorrected). Five thousand permutation tests were applied to assign a FWE corrected p -value to each connected component based on its size. The size of an effect was calculated based on its extent rather than intensity to find the number of edges comprised in the component (Baggio et al., 2018). For the correlation analysis, F-test was applied and the inflection point of each subject was the fixed effect of interest. Then, we investigated

differences of the connectivity between pwMS and controls in those subnetworks that were correlated with the inflection point. For group analysis, two sampled t test was used following the permuting test (5,000 permutation) controlling by FWE correction ($p < .05$) using NBS. Age and sex were used as adjusting covariates for the correlation analysis and group analysis. A threshold of t -score higher than 3.1 was used for cluster definition. For reporting, we visualized the association between selected nodes and edges and delayed access to consciousness with dot plots and simple regression estimates.

2.5.2 | Tract based spatial statistics

Tract based spatial statistics (TBSS) was performed to compare the whole brain fiber bundles between the groups by enabling the statistical evaluation of variations in the major white matter pathways voxel-by-voxel as described in Smith et al. (2006). Linear mixed models were applied to compare the mean FA of region of interests (ROI) that were drawn based on TBSS analysis and their correlations with the behavioral inflection point adjusting by age and sex. Please see Supporting Information *TBSS* for more detailed information.

2.5.3 | Structural connectivity between the clusters of altered functional activation

In addition to NBS analysis, we performed a post hoc analysis by calculating the structural connectivity only between those regions that showed an altered activation during the task. Briefly, we extracted the clusters, transformed them into the individual diffusion space, and performed probabilistic tractography as mentioned above. Again, we extracted mean FA of the streamlines as a measure of structural connectivity.

2.6 | Statistics

All analyses were performed using statistics in R 3.2.3 including the LMER (Bates, Mächler, Bolker, & Walker, 2015), the igraph (Csárdi & Nepusz, 2006), RootsExtremaInflections (Christopoulos, 2019) and inflection (Christopoulos, 2014) packages. We compared the age using Student t tests. Chi-square test with Yates's continuity correction was applied for the sex comparison. To investigate further comparisons and association between outcomes, we used linear mixed effect models corrected for age and sex and correcting for recurrent measurements in single patients (e.g., eyes). We extracted standardized beta values to compare the strength of association between outputs. For the group comparison of each contrast in the fMRI analysis, statistical factorial design specification was done in SPM12 involving two-sample t test adjusted by the two covariates age and sex. One-sample t test was also used for only the fixed effect analysis to see the general fMRI experiment pattern (i.e., whole SOA vs rest) in each group. All p values mentioned in the results section are corrected for multiple

comparisons either by FDR or FWE. FDR was applied and corrected p -values $<.05$ were considered as significant. FWE based on the random field theory provides more specific inference about topological features (i.e., cluster level) rather than voxel-wise FDR correction, while FDR provides more sensitive interpretation in domestic features (Chumbley & Friston, 2009). Therefore, we used FWE correction with $p < .05$ for the interpretation of the topological features of spatially extended fMRI signals and structural connectivity. For the individual level of multiple testing, we used FDR correction ($p < .05$).

3 | RESULTS

3.1 | Demographic information, visual functioning, and integrity of the anterior visual system

We recruited 30 pwMS with low to moderate disability and an average disease duration of 8 years since first symptoms. HC ($n = 34$) did not differ concerning age ($p = .559$) and sex ($p = .452$). pwMS were treated by fumarate, rituximab, interferon-beta, glatirameracetate, natalizumab, fingolimod, teriflunomid, alemtuzumab, ocrelizumab. Normative data were used to assess SDMT scores and the scores were on average 1.5 SD below the norm which might indicate a mild cognitive impairment. Thirteen of 30 pwMS had optic neuritis. When we compared eyes with and without a history of optic neuritis among these patients, we detected no differences for visual assessments, OCT and VEP (Figure S1 and Table S1). In addition, we observed no difference in SDMT performances between patients with and without optic neuritis ($p = .726$). Overall, pwMS had a slight impairment of visual functioning in comparison to HC: Besides a reduced LCVA (Sloan charts at 2.5%) ($p < .001$), we observed reduced AULCSF ($p = .003$), that is an estimate of visual acuity over the complete contrast and spatial frequency spectrum. However, HCVA at a distance of 5 m (Snellen) was not impaired. Moreover, we observed no prolonged VEP (i.e., indicating the transmission of signals from the retina to the primary visual cortex) in pwMS. Investigating structural retinal integrity with OCT, we detected no relevant loss of RNFL and GCIPL in comparison to controls. Descriptive statistics are given in Table 1.

3.2 | Behavioral performance and transition from unconscious to conscious processing

To determine performance and regional brain activation during conscious and unconscious processing of visual information, all participants performed the backward masking paradigm. The reaction time (rt) of pwMS was longer during late SOAs (>50 ms) ($rt_{pwMS} = 0.41 \pm 0.24$ s, $rt_{HC} = 0.33 \pm 0.20$ s, $p < .001$; Figure 2a) thus rather during conscious processing but not during unconscious processing ($rt_{pwMS} = 0.47 \pm 0.23$ s, $rt_{HC} = 0.47 \pm 0.22$ s, $p = .504$). The objective

performance revealed lower accuracy in pwMS over all SOA (pwMS 54.7%, HC 68.0%, $p < .001$, Figure 2b), that is, during unconscious and conscious processing. Moreover, we computed the delay between stimuli and mask that determines the transition from unconscious to conscious processing. At the group level, we determined the pwMS' inflection point (i.e., sudden increment of the performance that shows the access to conscious states) above a SOA of 50 ms, while HC showed conscious processing already above 16 ms after a short preconscious period (Figure 2c). On an individual level, the transition in controls occurred on average after 57.8 ms ($SD = 26.3$ ms) while we observed a significant later access in pwMS (mean = 74.2 ms, $SD = 23.6$ ms, $p = .014$). There were objective performances above chance during unconscious processing indicating subliminal processing (i.e., receiving the information without conscious awareness) (Figure 2c).

3.3 | Association between anterior visual system integrity and access to conscious processing in pwMS

Next, we explored whether the individual access threshold to consciousness was associated with important demographic and disease characteristics (Figure 3). In pwMS, the inflection point increased with longer disease duration ($p < .001$, $\beta = .37$) and disability ($p < .001$, $\beta = .24$), but showed no association with other typical MS disability outcomes including hand function and walking. Notably, neither visual acuity nor VEP or loss of retinal neural integrity was clearly associated with accuracy (Figure S2) or the inflection point (Figure 3). However, inflection point slightly differed between pwMS (mean = 83 ms, $SD = 20.8$ ms) and those without a history of optic neuritis (mean = 66 ms, $SD = 23.6$ ms), but this was only a tendency ($p = .05$). Please note that, the inflection point did not show a relation with SDMT performance (Figure 3). However, we observed a strong association between SDMT and accuracy ($p < .001$, $\beta = .39$) once pwMS accessed conscious processing, that is, if the delay between stimulus and mask was longer than 50 ms (Figure 4b), while there was no association for unconscious processing (SOA below 50 ms, $p = .056$, $\beta = -.072$, Figure 4a). In HC, we observed no correlation between the inflection point and any of the other outcomes.

3.4 | Brain activation differs between pwMS and controls for unconscious but not for conscious processing

Next, we analyzed BOLD signal fluctuations as an indicator of local brain activation during the task. Overall, the activation pattern was similar in pwMS and HC (Figure 5a,b): Anterior cingulate, precentral gyrus, thalamus, inferior parietal, and insular cortex were the main activated regions. To distinguish altered brain activation, we compared the contrast between pwMS and HC for conscious and unconscious processing separately. During unconscious processing, there

TABLE 1 Demographic and clinical information of people with MS and healthy controls

	MS N = 30 (19 RRMS, 8 PPMS, 3 SPMS)	HC N = 34	p value
Age years	44.1 (9.4)	45.4 (8.7)	.559
Sex (F/M)	15/15	20/14	.452
Education n (>12/<12 years)	17/13	-	-
Disease duration years	8.6 (6.4)	-	-
EDSS median (interquartile range)	2.5 (2.5)	-	-
Optic neuritis n	13	-	-
SDMT correct answers	57.3 (8.7)	-	-
SDMT SD of norm data	1.5	-	-
NHPT s	22.3 (4.8)	-	-
T25FW s	4.6 (1.5)	-	-
Low contrast visual acuity (Sloan charts at 2.5%) correct answers	17.9 (9.4)	28.2 (5.2)	<.001
High contrast visual acuity median (range)	0.95 (0.45–1.25)	1.0 (0.58–1.25)	.278
Area under the log contrast sensitivity function	1.10 (0.25)	1.28 (0.17)	.003
Visual evoked potential ms	118 (8.1)	113 (8.5)	.077
GCIPL volume mm ³	0.3 (0.02)	0.3 (0.02)	.482
Peripapillary RNFL thickness μm	12.1 (3.4)	11.2 (2.9)	.416
Total brain volume ml	1,590 (146)	1,543 (139)	.181
White matter volume ml	477 (57)	482 (57)	.691
Gray matter volume ml	653 (61)	648 (58)	.733

Note: Data are given as mean (SD) if not otherwise indicated. Group differences were compared with the student *t* test. Chi square test was used for sex comparison. SDMT values were reported as SD from available norm data adjusted for sex, age, and education. Results are FDR corrected. Bold *p* values indicate a significant difference between patients and controls.

Abbreviations: EDSS, expanded disability status scale; F/M, female/male; GCIPL, Ganglion cell/inner plexiform layer; HC, healthy controls; ml, milliliter; mm, millimeter; ms, millisecond; MS, multiple sclerosis; n, number; NHPT, nine hole peg test; PPMS, primary progressive MS; RNFL, retinal nerve fiber layer; RRMS, relapsing remitting MS; s, second; SD, standard deviation; SDMT, symbol digit modalities test; SPMS, secondary progressive MS; T25FW, time 25 food walk; μm, micrometer.

was decreased activation in bilateral precuneus (L; $p = .001$, R; $p = .038$), bilateral posterior cingulate gyrus (L; $p = .019$, R; $p = .032$), left middle ($p = .032$), and superior ($p = .024$) frontal gyrus, visual association area ($p = .038$) and extrastriate cortex ($p = .038$) in pwMS compared with HC (Figure 5c and Table 2). However, the groups did not differ during conscious processing.

3.5 | Regional loss of cortical thickness in not associated with delayed access to consciousness

After proving altered brain activation during unconscious processing in MS, we analyzed the association between behavioral results and altered brain structure. First, we determined the loss of gray matter by comparing cortical thickness between pwMS and HC. We found several regions with reduced cortical thickness, namely left caudal middle frontal, lateral occipital, inferior temporal, lingual, precuneus, and right inferior parietal, isthmus of the cingulate gyrus, precentral and parahippocampal cortex ($p < .001$, Figure S3A). However, there was no correlation between cortical thickness and the inflection point in MS (Figure S3B).

3.6 | Structural connections associated with the time to access conscious processing

Global structural connectivity was lower in pwMS compared with controls ($p = .003$, Figure S4). Lower global connectivity was correlated with longer access to consciousness in pwMS ($r = -.38$, $p = .042$, Figure S4). In contrast, we found positive correlation between global structural connectivity and inflection point in controls ($r = .52$, $p < .001$, Figure S4).

Next, we investigated which connections or subnetworks are associated with delayed access to conscious processing in pwMS. First, we extracted subnetworks that were correlated with the individual inflection point separately for each group. Here, we identified a widespread subnetwork with the same 38 nodes in both groups and a close overlap of edges (HC: 488, pwMS: 460; Figure S5 for pwMS; Table S2). In a second step, we applied NBS again to determine which of the connections in this subnetwork differed significantly between the groups. We identified a smaller network with 12 nodes and 10 edges with reduced structural connectivity in pwMS in comparison to HC (Figure 6a). This network included the primary visual cortex, subcortical gray matter, cortical areas associated with the so-called

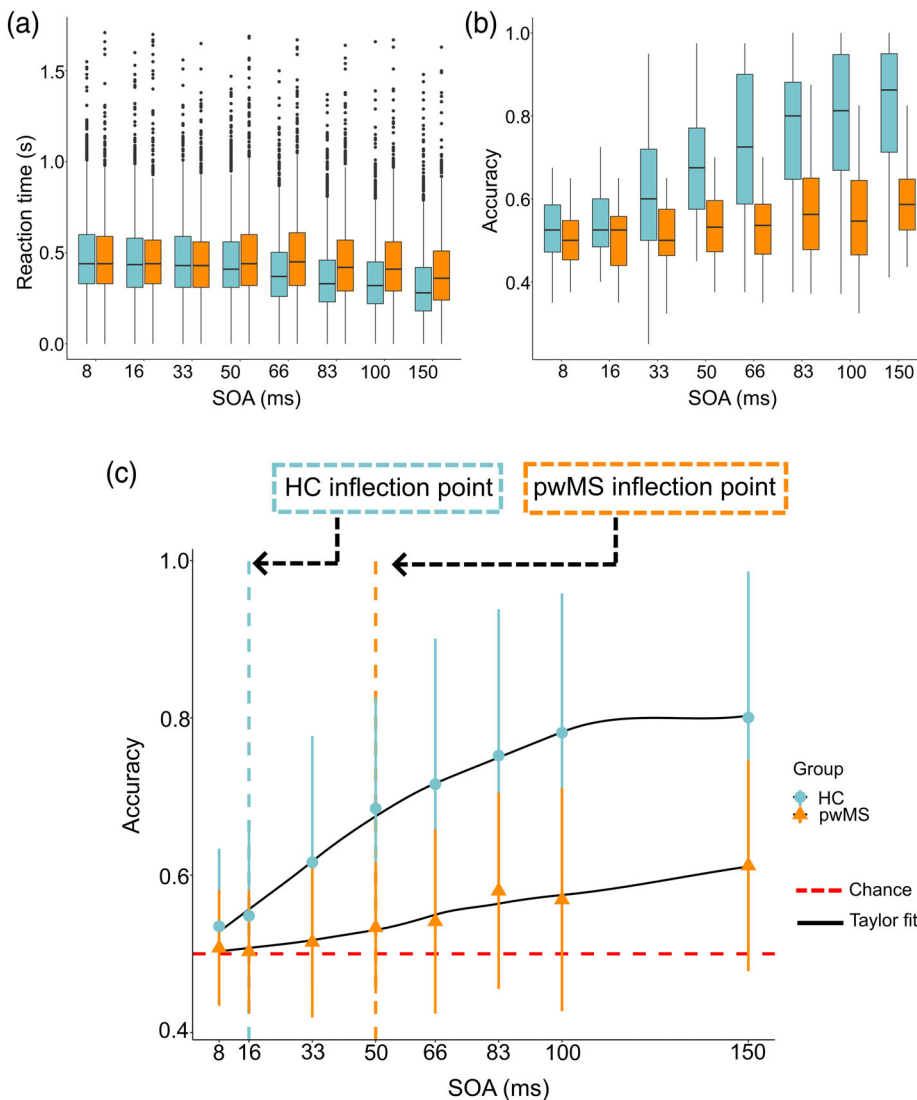


FIGURE 2 Distinction between unconscious and conscious processing. (a) Reaction time within the 2 s trial duration for each stimulus onset asynchrony (SOA) during the fMRI experiment is given for pwMS (orange) and healthy controls (blue). (b) Objective performance (accuracy) obtained during fMRI experiment is shown for each SOA. Accuracy is given as a percentage of correct answer of comparison the target number with 5. (c) Objective performance obtained during fMRI experiment is plotted as a nonlinear function of stimulus onset asynchrony (SOA) which is seen as black lines. Dashed lines show the inflection point for controls (blue) and pwMS (orange). Horizontal red dashed line indicates chance point. Accuracy is given as a percentage of the correct answer of comparison the target number with 5 at 8 different SOAs. Blue circle and orange triangle indicate median of the objective performance at each SOA for healthy controls and pwMS

dorsal stream, and insular areas (Figure 6a). Progressive loss of node connectivity (Figure 6b) and edge strength (Figure 6c), defined as the difference between individual strength in patients and mean values from controls, were related with longer time to access consciousness. On the nodal level, three of the top four correlated nodes were located in the primary visual area, including right occipital pole ($r = -.39$, $p = .029$), left occipital middle ($r = -.38$, $p = .038$) and right occipital superior gyrus ($r = -.38$, $p = .037$) (Figure 6b). Precuneus as the fourth node is rather part of the unconscious processing pathway in the dorsal stream (left precuneus, $r = -.37$, $p = .045$, Figure 6b). On an edge level, the inflection point correlated strongest with the connection between a primary visual area (right superior occipital gyrus) and the insula (right circular inferior insula sulcus) ($r = -.39$, $p < .050$ FDR corrected, Figure 6c).

We also wanted to show the regional change of whole brain white matter bundles and the relationship between the mean FA of the ROIs specified based on the regional changes and behavioral inflection point. There was widespread lower FA in MS compared with controls, such as bilateral inferior fronto-occipital fasciculus (IFOF), inferior longitudinal fasciculus (ILF), uncinate fasciculus,

superior longitudinal fasciculus, anterior thalamic radiation, optic radiation, genu, body and splenium of the corpus callosum (CC) (Figure 7a, $p < .05$ FWE corrected). Notable, we found that lower FA in the splenium of CC was negatively correlated with the behavioral inflection point (i.e., lower FA indicates longer access to consciousness; $p = .035$, $\beta = -.37$, Figure 7b) in MS. Controls did not show such correlation in splenium of CC; however, there was negative correlation between the behavioral inflection point and right anterior thalamic radiation ($p = .030$, $\beta = -.36$) as well as positive correlation with right IFOF ($p = .029$, $\beta = .36$) in controls (Figure 7b).

In addition, we performed a post hoc analysis investigating the association between the inflection point and the strength of connectivity between those brain regions that have shown a decreased activation during the unconscious part of the fMRI task. However, connection strength as estimated with mean FA values was not correlated with the inflection point, neither in pwMS nor in controls.

4 | DISCUSSION

In our cohort of pwMS, unconscious processing was associated with lower activation in both dorsal and ventral stream, but an association

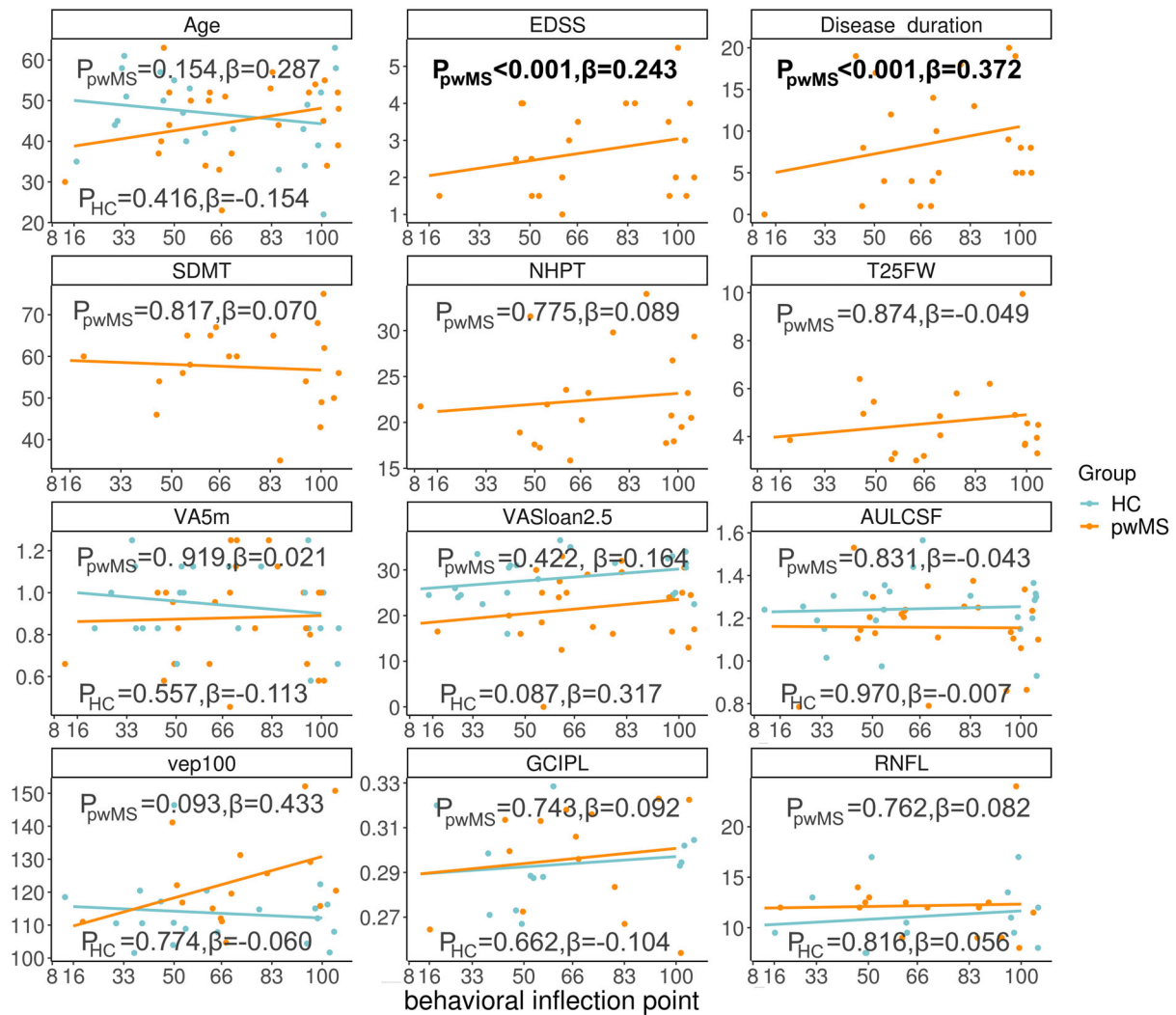


FIGURE 3 Access to conscious processing in people with Multiple Sclerosis (pwMS) correlates with disability and disease duration but not with anterior visual system integrity. Relationship between individual behavioral inflection point and neurological and visual assessments. X axis represents the behavioral inflection point. Y axis indicates the measured values of a specific assessment given as title of each graph. Age and disease duration after first syndrome are given in years. Orange and blue indicate pwMS and healthy controls, respectively. EDSS = expanded disability status scale; SDMT = symbol digit modalities test; NHPT = nine hole peg test; T25FW = time 25 food walk; VA5m = high contrast visual acuity; VASloan2.5 = low contrast visual acuity (Sloan charts at 2.5%), AULCSF = the area under the log contrast sensitivity function; VEP100 = visual evoked potential, GCIPL = ganglion cell/inner plexiform layer; RNFL = retinal nerve fiber layer

with disrupted structural connectivity was only detected within the dorsal stream. Here, unconscious performance was independent from conscious information processing and structurally not linked to cortical thinning. Moreover, we observed no strong association between affection of the anterior visual system and conscious access during a task with a high demand on fast visual input processing. In contrast, loss of structural connectivity between the primary visual and insula reflected the strongest association with the delay in conscious perception in pwMS. Overall, our study indicates that the transition from unconscious to conscious processing of visual information is impaired in MS and that it seems to be associated with reduced structural connectivity between primary visual areas and high-level regions. However, the overall performance of upstream pathways including the anterior visual system seems rather robust against MS pathology.

Here, we could confirm previous MS studies (Reuter et al., 2007, 2009) showing delayed conscious access in MS. This supports the idea that the unconscious processing is important for MS. In our MS cohort, the delay was independent from the general cognitive performance as estimated with the SDMT—a common test to evaluate cognition in pwMS (Nygaard et al., 2015). Visual and hand functioning did not show an effect on the task. Since the unconscious thought affects the real-life events such as decision-making, judgments, attitude formation, impression formation, driving and creativity (Dijksterhuis, 2019; Dijksterhuis & Strick, 2016; Ito & Yamazaki, 2016), exploring unconscious processing might be useful for counseling pwMS. Block (Block, 2005) clarified the term “access consciousness” by addressing the fact that, conscious information is accessible to various cognitive processors (i.e., working memory, motor behavior, or verbal reporting)

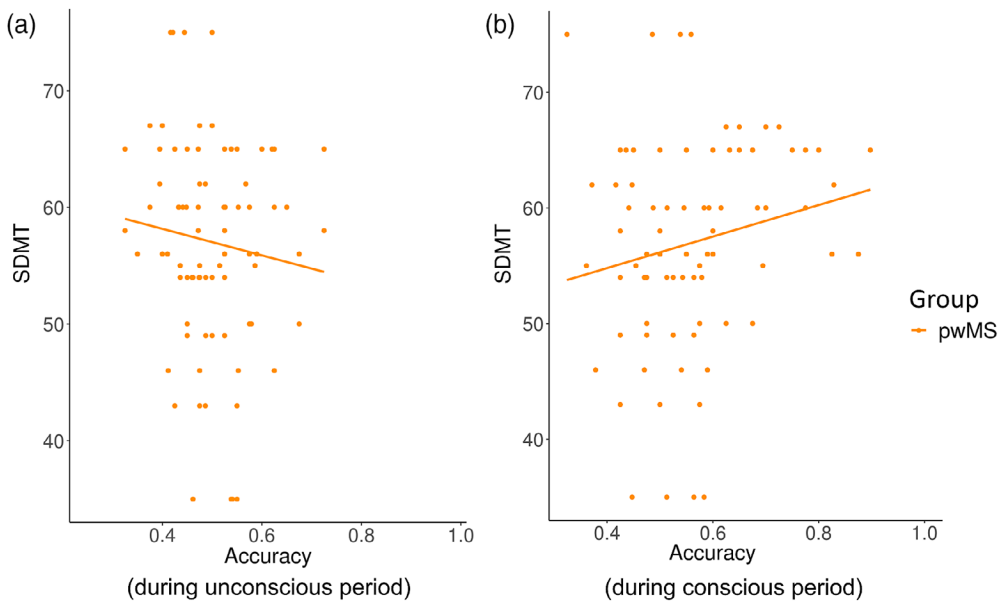


FIGURE 4 SDMT correlates only with task accuracy during consciousness in pwMS. (a) Lack of association between the accuracy obtained during unconscious processing (SOA ≤ 50) and SDMT scores. (b) SDMT shows a strong correlation with the accuracy of patient ($p < .001$, $\beta = .39$) during consciousness of pwMS (SOA > 50 ms)

in contrast to unconscious information. The distinctions are also explained by two theories such as global neuronal workspace (GNW) (Mashour, Roelfsema, Changeux, & Dehaene, 2020) and information integration theory (IIT) (Tononi, Boly, Massimini, & Koch, 2016), suggesting that unconscious process is local and encapsulated while conscious process is interactive by global broadcasting to other processors. In line with previous findings, SDMT was related to accuracy during consciousness, but did not cover unconscious processing. Moreover, we observed an association with disease duration and disability indicating a progressive loss of conscious access abilities in MS. Taken together, the behavioral results of our study suggest that unconscious processing of information, represents an independent dimension of cognitive functions in pwMS.

In our study, there was decreased activation only during unconscious processing. Specifically, visual, precuneus, posterior cingulate and frontal areas showed reduced activation during unconscious processing of the information, which makes sense because the superior frontal and intraparietal cortex interacts with the dorsal stream during normal vision to divert the attention to the unexpected or salience events (Corbetta & Shulman, 2002). In addition, these regions are part of the default mode network which is de-activated during cognitive tasks, but active during rest (Buckner & DiNicola, 2019). The importance of the DMN for understanding cognitive impairment in MS has been described before (Rocca et al., 2017; van Geest et al., 2018; Veréb et al., 2020) and lower activity of DMN regions (i.e., middle and superior frontal, superior temporal, precuneus, cingulate gyrus) has been also considered as an indicator of conscious impairment (Crone et al., 2011) and as well as information processing speed (Chen et al., 2020; van Geest et al., 2018). In our MS cohort, decreased activation in DMN regions was peculiar to unconscious processing and not detectable during conscious processing. These regions are known as responsible for encoding the specific information even before they enter consciousness (Soon, He, Bode, & Haynes, 2013). In addition, since the prefrontal cortex, precuneus and

cingulate cortex are known to rule and maintain conscious processing as well as control of behavior, the reduction of their functionality may lead to delayed consciousness in pwMS (Luppi et al., 2019; Panagiotaropoulos, Dwarakanath, & Kapoor, 2020; Van Gaal & Lamme, 2012). Although these regions have their own functionality and specificity, they are also densely connected with each other (Bartfelda et al., 2015; Markov et al., 2013). However, they seem also especially vulnerable to MS pathology (Stellmann et al., 2017). Therefore, any information detected by one of them may activate the others quickly and the disruption of one of these hubs may cause a serial decreased activation resulting as disrupted unconscious processing of information. Further studies may investigate direct association between the functional activation and dynamic β change of the connectivity that are correlated with unconscious processing of the information.

Here, global structural connectivity was associated with task performance and delayed access to consciousness in MS. However, such an association indicates that both parameters are progressively altered with disease severity and provide no specific information. Focal lesions do not cause complete loss of conscious processing but it disrupts the neurons or their interconnectivity that are relied on GNW (Mashour et al., 2020). In MS, focal lesions in the visual system (for example optic neuritis or focal lesion in the visual tracts) can lead to altered functional connectivity of the visual system and translate into long-range neurodegeneration through trans-synaptic degeneration (Backner et al., 2018; Gabilondo et al., 2014). The only MS study conducted in very early MS patients with normal VEP showed that the damage was mainly located in the right dorsolateral frontal fasciculus and occipito-frontal fasciculus (Reuter et al., 2009). Even though we also found a relation between the inflection point and right inferior fronto-occipital fasciculus in healthy controls, we observed no strong association between delayed access to conscious processing and disrupted structural connectivity in frontal regions in our cohort of pwMS. Instead, we located strong damage in splenium of corpus

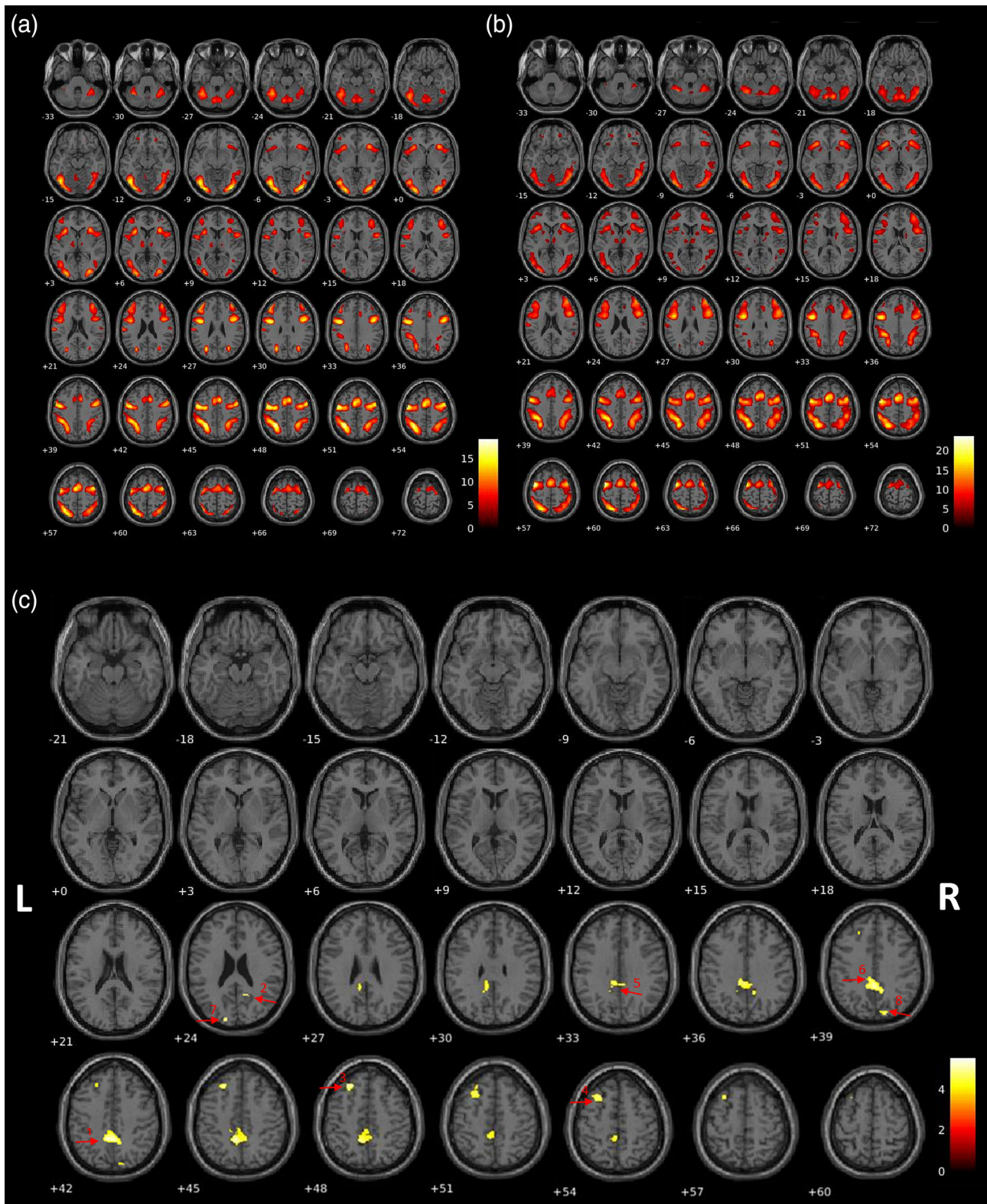


FIGURE 5 Brain activation differs between people with Multiple Sclerosis (pwMS) and healthy controls for unconscious but not for conscious processing. (a) Fixed effect of the masking experiment specified as whole SOA versus rest in pwMS. Red-yellow areas show the brain regions activated by masking experiment in pwMS (FWE corrected). (b) Fixed effect of the masking experiment specified as whole SOA versus rest in healthy controls (HC). Red-yellow areas show the brain regions activated by masking experiment in HC (FWE corrected). (c) Comparison of the contrasts of unconscious and neutral (1–1) between pwMS (SOA \leq 50) and HC (SOA \leq 16 ms). Decreased activation (yellow) during unconscious processing in pwMS compared with HC. Numbers that are shown by red arrows are indicating the significant regions given in Table 2. Displayed in “neurological” convention, That is, the left hemisphere is shown on the left. L = Left hemisphere; R = Right hemisphere

TABLE 2 Decreased functional activation during unconscious processing during the visual backward masking experiment versus fixation periods in people with MS compared with healthy controls

Number	Region	Functional system	<i>p</i> (FWE-corr)	<i>k</i>	Peak Z	Peak T	MNI coordinates (mm)		
1	Left precuneus	Dorsal stream	.001	146	5.53	4.99	-6	-46	44
2	Right precuneus	Dorsal stream	.038	17	5.01	4.59	14	-59	26
3	Left superior frontal gyrus	Frontal	.024	21	5.25	4.77	-24	32	48
4	Left middle frontal gyrus	Frontal	.032	21	5.07	4.64	-26	20	54
5	Right posterior cingulate cortex	Limbic	.032	17	5.05	4.62	2	-34	33
6	Left posterior cingulate gyrus	Limbic	.019	6	5.12	4.68	-6	-36	38
7	Occipital cortex (visual association area)	Primary visual	.038	24	5.00	4.58	-14	-90	24
8	Occipital lobe (extrastriate cortex)	Primary visual	.038	22	4.98	4.57	18	-82	39

Note: Brain regions exhibiting a significant contribution ($p < .050$ corrected at cluster level; $k > 0$ voxels; threshold at voxel-level: $p < .050$ FWE-corrected) to the decreased activation. The peaks within each identified cluster of activity are given as T and Z values. The numbers indicating regions are the same as in Figure 2c.

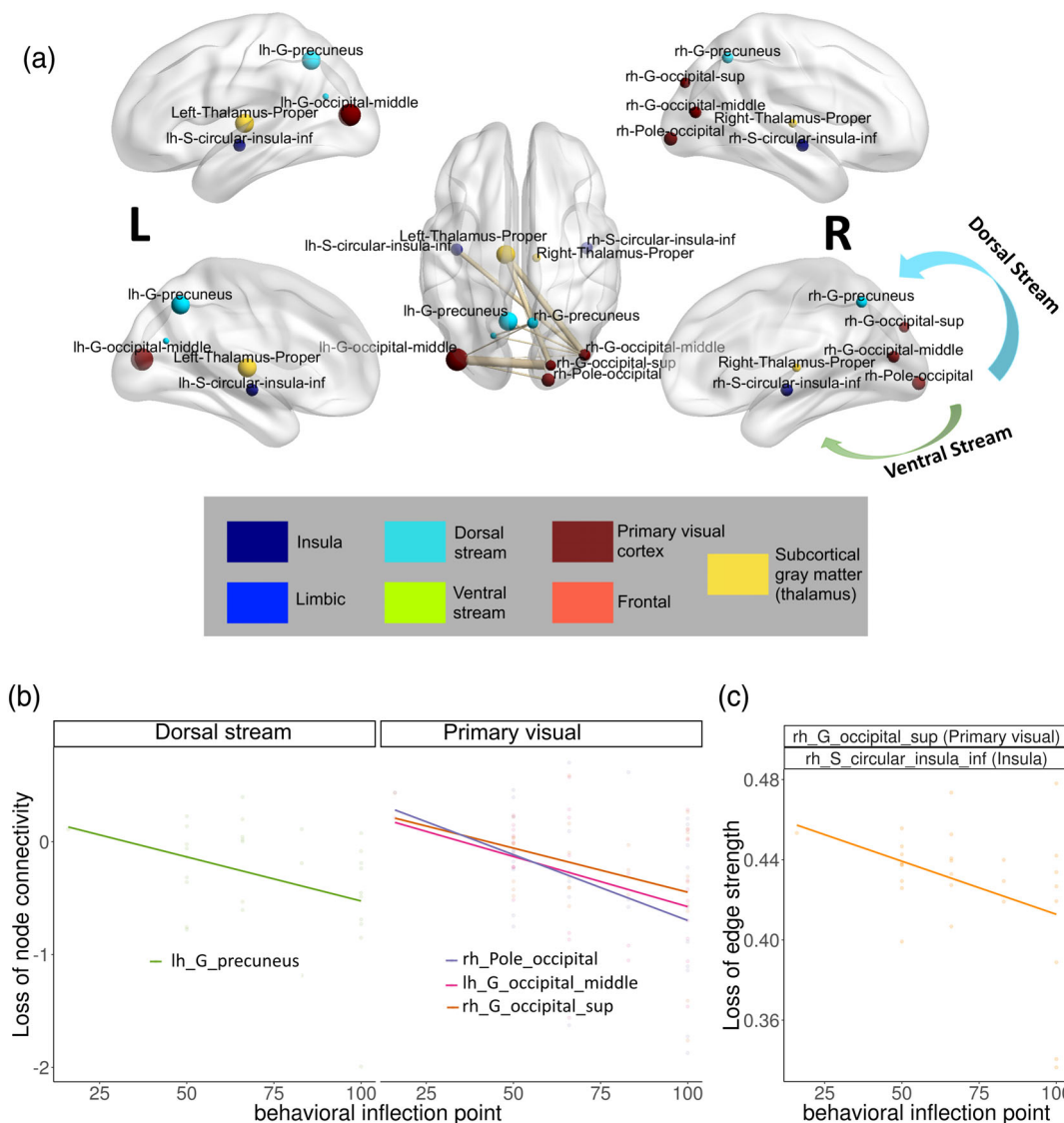


FIGURE 6 Structural connections associated with the time to access conscious processing. (a) Subnetworks of edges and nodes that show a correlation with access to consciousness (inflection point) and differ between patients and controls. BrainNet plots illustrate the localization of highly correlated ($t > 3.1$, $p < .050$) nodes in the brain. The color bar describes whether a node belongs to the visual system or not (based on the location). L = Left hemisphere; R = Right hemisphere. (b) Top 4 out of 10 correlations between the inflection point and the loss of connectivity of the nodes in patients. Loss of strength quantified by subtracting mean values from controls from individual values in pwMS. (c) Only one correlation between the inflection point and the edge strength (connections; pwMS–mean (HC))

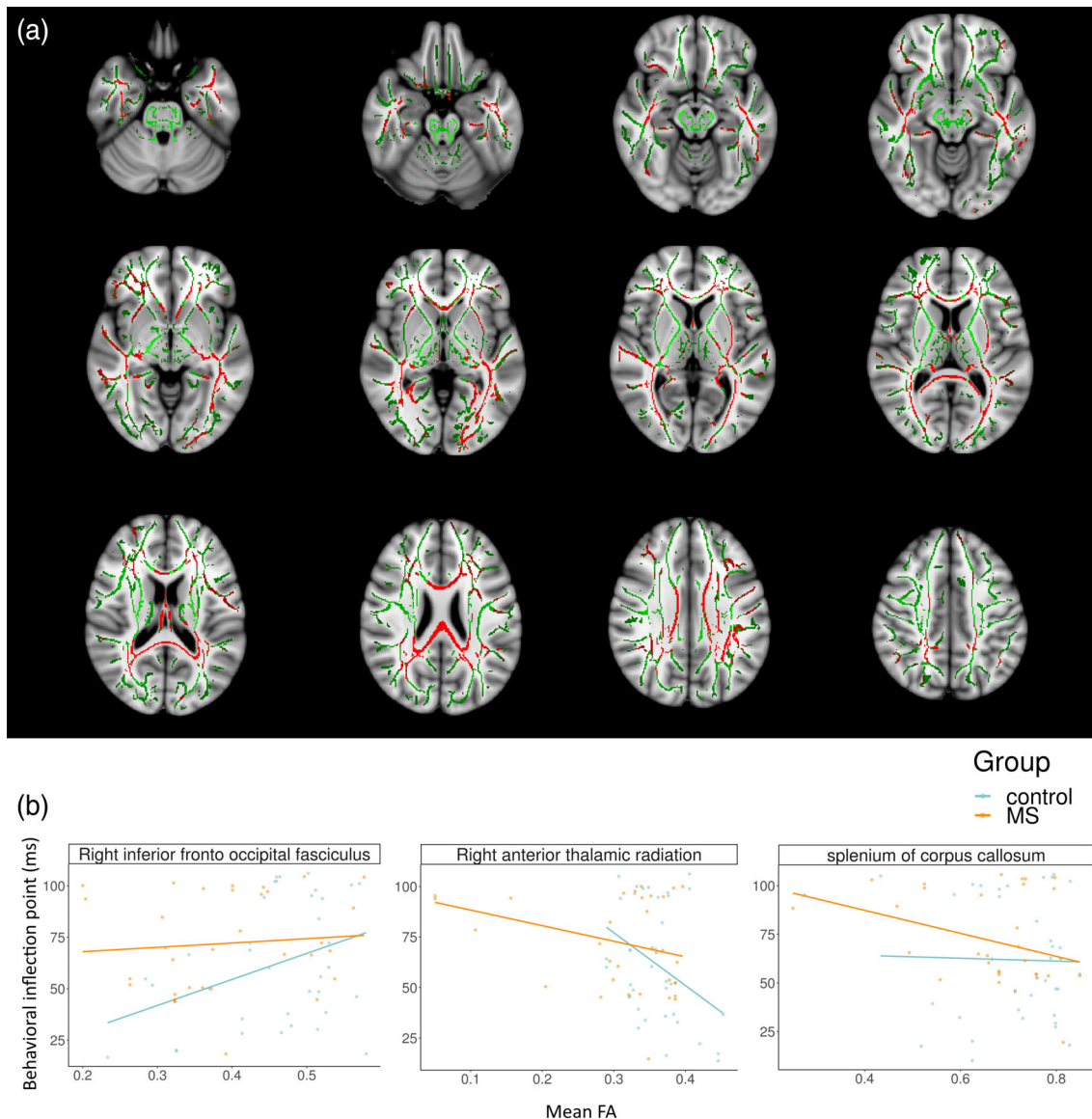


FIGURE 7 Lower fractional anisotropy in people with Multiple Sclerosis (pwMS) is related with longer access to consciousness. (a) Widespread lower fractional anisotropy (FA) in pwMS compared with controls. Green color indicates mean FA skeleton, red indicates lower FA in pwMS than controls. (b) Correlation between mean FA of each ROI and the behavioral inflection point (only significant correlation is illustrated)

callosum related to longer access to consciousness in pwMS. In addition, decreased connectivity between the right primary visual area and the insula was correlated with later access to consciousness in pwMS. Visual information are transferred from the right to left hemisphere via the CC (i.e., a bridge between two hemispheres) (Volz & Gazzaniga, 2017). Damage in the right hemisphere effects both intra-hemispheric and interhemispheric connections related to self-awareness (Morin, 2017). Daini (2019) states that the consciousness not only rely on the hemispheric damages, but also on the integrity of corpus callosum that can cause the lack of access to left hemisphere. The most posterior part of the CC, the splenium, plays a crucial role in consciousness because of its location (i.e., connecting occipital, posterior parietal and inferior temporal cortices of the left and right hemispheres) and fiber composition (i.e., the posterior splenium has thicker

fibers that combine the hemi-representation of the visual field) (Blaauw & Meiners, 2020). In splenial pathology, the lack of information transfer (i.e., visuospatial or auditory) between the occipito-temporal-parietal cortices of both hemisphere along with disruption of cerebral networks can differ the consciousness (Blaauw & Meiners, 2020). Consistently, impaired cerebral network between primary visual-insula in the right hemisphere along with the damage in the splenium of CC might cause delayed conscious access in MS.

Several limitations of our small and cross-sectional study have to be considered. The sample size restricted our ability to detect difference for certain outcomes such as for OCT between the eye with and without a history of ON. Nevertheless, we used multiple comparison correction (Chen, Lu, & Yan, 2018). Moreover, we did not include a formal testing of handedness, which may influence the performance,

especially the reaction time. However, responses during the task were randomly and equally distributed on both hands, there was no reaction time difference between the hands, and we used accuracy not reaction time as the main outcome. Nevertheless, we cannot rule out that handedness might have partially influenced our fMRI results in the motor system. In addition, neuropsychological assessment was limited by using only the SDMT which is mainly a test for information processing speed and might have missed impairment in other cognitive domains. However, SDMT is widely accepted as valuable screening test in MS and can thus be considered as informative with regard to the overall cognitive performance (Benedict et al., 2017). In addition, the lack of some clinical evaluation of controls limited the identification of impairments such as hand functioning or SDMT. We did not control the results with education information likewise previous studies, which may cause a limitation. The task was designed to measure only objective performance (accuracy). Even though it is known that accuracy is highly correlated with subjective rating of consciousness (Reuter et al., 2007, 2009), the objective inflection point remains a proxy of the true threshold that can only be determined subjectively. We were not able to perform functional connectivity analysis in the current study, further studies may look into this issue further. The study was limited in highlighting the positive correlations in healthy controls. In a recent study, it has been claimed that there is a negative correlation between the conscious access threshold and structural connectivity within the predefined GNW theory bundles when the groups (controls and patients) are combined (Berkovitch et al., 2021). However, our study was not designed to investigate the impact of structural connectivity on conscious access in healthy individuals. The lower performance at higher connectivity might indicate a less efficient organization of the network (Meijer, Steenwijk, Douw, Schonheim, & Geurts, 2020).

In our study, pwMS showed delayed conscious access, seen as a decrease activation during unconscious processing compared with controls. Prolonged conscious access was related with lower structural connection between primary visual and insula in the right hemisphere and decreased FA in the splenium of CC. Taken together, prolonged conscious access correlates rather with structural connectivity between primary visual areas and high-level cortical regions than on the anterior visual system in MS. Moreover, a reduced activation pattern during unconscious processing of visual information showed an overlap with the default mode network, which has been linked to several cognitive functions in MS. This is important for MS because disrupted unconscious processes seems to be involved in the pattern of cognitive functions and that may explain the difficulties in daily life experience of pwMS. Our study indicates that the impaired transition of unconscious stimuli to conscious processing seems relevant in MS and could be also important for other cognitive domains such as attention and working memory.

ACKNOWLEDGMENTS

The study was partially funded by a grant from Genzyme to JPS. Open Access funding enabled and organized by Projekt DEAL.

CONFLICT OF INTEREST

Stefan M. Gold receives personal fees from Almirall S. A., Celgene, Forum für Medizinische Fortbildung (FomF) and Mylan GmbH, and is in-kind research contributions from GAIA Group, Jan-Patrick Stellmann receives partial foundation from Genzyme. Other authors have nothing to declare.

AUTHOR CONTRIBUTIONS

Arzu C. Has Silemek, Jean-Philippe Ranjeva, Bertrand Audoin, and Jan-Patrick Stellmann designed research; Arzu C. Has Silemek performed research; Arzu C. Has Silemek and Jan-Patrick Stellmann analyzed data; and Arzu C. Has Silemek, Jean-Philippe Ranjeva, Bertrand Audoin, Martin Weygandt, Christoph Heesen, Simone Kühn, Stefan M. Gold, and Jan-Patrick Stellmann wrote and revised the paper.

ETHICS STATEMENT

Ethical approval was obtained from the local ethic committee of Hamburg Chamber of Physicians (Registration Number PV5557). Institutional Review Board (IRB) was taken and all participants gave written informed consent prior to any testing under this protocol.

DATA AVAILABILITY STATEMENT

The data that support the findings of this study are available from the corresponding author upon reasonable request.

ORCID

Arzu C. Has Silemek  <https://orcid.org/0000-0003-4609-0956>
 Jean-Philippe Ranjeva  <https://orcid.org/0000-0001-8073-102X>
 Simone Kühn  <https://orcid.org/0000-0001-6823-7969>
 Martin Weygandt  <https://orcid.org/0000-0001-9962-4582>
 Jan-Patrick Stellmann  <https://orcid.org/0000-0003-2565-2833>

REFERENCES

- Ansorge, U., Kunde, W., & Kiefer, M. (2014). Unconscious vision and executive control: How unconscious processing and conscious action control interact. *Consciousness and Cognition*, 27, 268–287. <https://doi.org/10.1016/j.concog.2014.05.009>
- Ashburner, J., Barnes, G., Chen, C., Daunizeau, J., Moran, R., Henson, R., ... Phillips, C. (2013). SPM12 manual the FIL methods group (and honorary members). *Functional Imaging Laboratory*, 15, 475–471. <https://doi.org/10.1111/j.1365-294X.2006.02813.x>
- Backman, C., Cork, S., Gibson, D., & Parsons, J. (1992). Assessment of hand function: the relationship between pegboard dexterity and applied dexterity. *Canadian Journal of Occupational Therapy*, 59(4), 208–213.
- Backner, Y., Kuchling, J., Massarwa, S., Oberwahrenbrock, T., Finke, C., Bellmann-Strobl, J., ... Levin, N. (2018). Anatomical wiring and functional networking changes in the visual system following optic neuritis. *JAMA Neurology*, 75(3), 287–295. <https://doi.org/10.1001/jamaneurol.2017.3880>
- Baggio, H. C., Abos, A., Segura, B., Campabadal, A., Garcia-Diaz, A., Uribe, C., ... Junque, C. (2018). Statistical inference in brain graphs using threshold-free network-based statistics. *Human Brain Mapping*, 39(6), 2289–2302. <https://doi.org/10.1002/hbm.24007>
- Balcer, L. J., Miller, D. H., Reingold, S. C., & Cohen, J. A. (2015). Vision and vision-related outcome measures in multiple sclerosis. *Brain*, 138, 11–27. <https://doi.org/10.1093/brain/awu335>

- Barttfeld, P., Uhriga, L., Sitta, J. D., Sigmans, M., Jarraya, B., & Dehaene, S. (2015). Signature of consciousness in the dynamics of resting-state brain activity. *Proceedings of the National Academy of Sciences of the United States of America*, 112(3), 887–892. <https://doi.org/10.1073/pnas.1418031112>
- Bates, D., Mächler, M., Bolker, B., & Walker, S. (2015). Fitting linear mixed-effects models using *lme4*. *Journal of Statistical Software*, 67(1), 1–48. <https://doi.org/10.18637/jss.v067.i01>
- Behrens, T. E. J., Berg, H. J., Jbabdi, S., Rushworth, M. F. S., & Woolrich, M. W. (2007). Probabilistic diffusion tractography with multiple fibre orientations: What can we gain? *NeuroImage*, 34(1), 144–155. <https://doi.org/10.1016/j.neuroimage.2006.09.018>
- Benedict, R. H. B., Deluca, J., Phillips, G., LaRocca, N., Hudson, L. D., & Rudick, R. (2017). Validity of the symbol digit modalities test as a cognition performance outcome measure for multiple sclerosis. *Multiple Sclerosis*, 23, 721–733. <https://doi.org/10.1177/1352458517690821>
- Berkovitch, L., Del Cul, A., Maheu, M., & Dehaene, S. (2018). Impaired conscious access and abnormal attentional amplification in schizophrenia. *NeuroImage: Clinical*, 18, 835–848. <https://doi.org/10.1016/j.nicl.2018.03.010>
- Berkovitch, L., Charles, L., Del Cul, A., Hamdani, N., Delavest, M., Sarrazin, S., ... Houenou, J. (2021). Disruption of conscious access in psychosis is associated with altered structural brain connectivity. *The Journal of Neuroscience: The Official Journal of the Society for Neuroscience*, 41(3), 513–523. <https://doi.org/10.1523/JNEUROSCI.0945-20.2020>
- Besson, P., Dinkelacker, V., Valabregue, R., Thivard, L., Leclerc, X., Baulac, M., ... Dupont, S. (2014). Structural connectivity differences in left and right temporal lobe epilepsy. *NeuroImage*, 100, 135–144. <https://doi.org/10.1016/j.neuroimage.2014.04.071>
- Blaauw, J., & Meiners, L. C. (2020). The splenium of the corpus callosum: Embryology, anatomy, function and imaging with pathophysiological hypothesis. *Neuroradiology*, 62(5), 563–585. <https://doi.org/10.1007/s00234-019-02357-z>
- Block, N. (2005). Two neural correlates of consciousness. *Trends in Cognitive Sciences*, 9(2), 46–52. <https://doi.org/10.1016/j.tics.2004.12.006>
- Bowring, A., Maumet, C., & Nichols, T. E. (2019). Exploring the impact of analysis software on task fMRI results. *Human Brain Mapping*, 40(11), 3362–3384. <https://doi.org/10.1002/hbm.24603>
- Breitmeyer, B., & Ogmen, H. (2010). *Visual masking: Time slices through conscious and unconscious vision*. Oxford, England: Oxford University Press. <https://doi.org/10.1093/acprof:oso/9780198530671.001.0001>
- Breitmeyer, B. G., & Ogmen, H. (2000). Recent models and findings in visual backward masking: A comparison, review, and update. *Perception & Psychophysics*, 62(8), 1572–1595. <https://doi.org/10.3758/BF03212157>
- Bruce, J. M., Bruce, A. S., & Arnett, P. A. (2007). Mild visual acuity disturbances are associated with performance on tests of complex visual attention in MS. *Journal of the International Neuropsychological Society*, 13(3), 544–548. <https://doi.org/10.1017/S1355617707070658>
- Buckner, R. L., & DiNicola, L. M. (2019). The brain's default network: Updated anatomy, physiology and evolving insights. *Nature Reviews Neuroscience*, 20, 593–608. <https://doi.org/10.1038/s41583-019-0212-7>
- Chan, T. (2000). An investigation of finger and manual dexterity. *Perceptual and Motor Skills*, 90(2), 537–542. <https://doi.org/10.2466/pms.2000.90.2.537>
- Chen, M. H., Wylie, G. R., Sandroff, B. M., Dacosta-Aguayo, R., DeLuca, J., & Genova, H. M. (2020). Neural mechanisms underlying state mental fatigue in multiple sclerosis: A pilot study. *Journal of Neurology*, 267(8), 2372–2382. <https://doi.org/10.1007/s00415-020-09853-w>
- Chen, X., Lu, B., & Yan, C.-G. (2018). Reproducibility of R-fMRI metrics on the impact of different strategies for multiple comparison correction and sample sizes. *Human Brain Mapping*, 39(1), 300–318. <https://doi.org/10.1002/hbm.23843>
- Christopoulos, D. (2014). Roots, Extrema and inflection points by using a proper Taylor regression procedure. *SSRN Electronic Journal*. <https://doi.org/10.2139/ssrn.2521403>
- Christopoulos, D. (2019). New methods for computing extremes and roots of a planar curve: introducing Noisy Numerical Analysis New methods for computing extremes and roots of a planar curve: introducing Noisy Numerical Analysis. <https://doi.org/10.13140/RG.2.2.17158.32324>
- Chumbley, J. R., & Friston, K. J. (2009). False discovery rate revisited: FDR and topological inference using Gaussian random fields. *NeuroImage*, 44(1), 62–70. <https://doi.org/10.1016/j.neuroimage.2008.05.021>
- Corbetta, M., & Shulman, G. L. (2002). Control of goal-directed and stimulus-driven attention in the brain. *Nature Reviews Neuroscience*, 3(3), 201–215. <https://doi.org/10.1038/nrn755>
- Crone, J. S., Ladurner, G., Höller, Y., Golaszewski, S., Trinka, E., & Kronbichler, M. (2011). Deactivation of the default mode network as a marker of impaired consciousness: An fMRI study. *PLoS One*, 6(10), e26373. <https://doi.org/10.1371/journal.pone.0026373>
- Csárdi, G., & Nepusz, T. (2006). The igraph software package for complex network research. *InterJournal Complex Systems*, 1695(5), 1–9. Retrieved from <https://pdfs.semanticscholar.org/1d27/44b83519657f5f2610698a8ddd177ced4f5c.pdf>
- Custers, R., & Aarts, H. (2010). The unconscious will: How the pursuit of goals operates outside of conscious awareness. *Science. American Association for the Advancement of Science.*, 329, 47–50. <https://doi.org/10.1126/science.1188595>
- Daini, R. (2019). The lack of self-consciousness in right brain-damaged patients can be due to a disconnection from the left interpreter: The DiLeI theory. *Frontiers in Psychology*, 10, 349. <https://doi.org/10.3389/fpsyg.2019.00349>
- Dehaene, S., Naccache, L., Cohen, L., Le Bihan, D., Mangin, J. F., Poline, J. B., & Rivière, D. (2001). Cerebral mechanisms of word masking and unconscious repetition priming. *Nature Neuroscience*, 4(7), 752–758. <https://doi.org/10.1038/89551>
- Del Cul, A., Baillet, S., & Dehaene, S. (2007). Brain dynamics underlying the nonlinear threshold for access to consciousness. *PLoS Biology*, 5(10), 2408–2423. <https://doi.org/10.1371/journal.pbio.0050260>
- DeLuca, J., Chiaravalloti, N. D., & Sandroff, B. M. (2020). Treatment and management of cognitive dysfunction in patients with multiple sclerosis. *Nature Reviews Neurology. Nature Research.*, 16, 319–332. <https://doi.org/10.1038/s41582-020-0355-1>
- Destrieux, C., Fischl, B., Dale, A., & Halgren, E. (2010). Automatic parcellation of human cortical gyri and sulci using standard anatomical nomenclature. *NeuroImage*, 53(1), 1–15. <https://doi.org/10.1016/j.neuroimage.2010.06.010>
- Diaz, M. T., & McCarthy, G. (2007). Unconscious word processing engages a distributed network of brain regions. *Journal of Cognitive Neuroscience*, 19(11), 1768–1775. <https://doi.org/10.1162/jocn.2007.19.11.1768>
- Dijksterhuis, A. (2019). *The Unconscious. Introduction to Psychology* (pp. 394–401). Saskatoon, Canada: University of Saskatchewan Open Press. Retrieved from <https://openpress.usask.ca/introductiontopsychology/>
- Dijksterhuis, A., & Nordgren, L. F. (2006). A theory of unconscious thought. *Perspectives on Psychological Science*, 1(2), 95–109. <https://doi.org/10.1111/j.1745-6916.2006.00007.x>
- Dijksterhuis, A., & Strick, M. (2016). A case for thinking without consciousness. *Perspectives on Psychological Science*, 11(1), 117–132. <https://doi.org/10.1177/1745691615615317>
- Fischl, B., Salat, D. H., Busa, E., Albert, M., Dieterich, M., Haselgrove, C., ... Dale, A. M. (2002). Whole brain segmentation: Automated labeling of neuroanatomical structures in the human brain. *Neuron*, 33(3), 341–355. Retrieved from <http://www.ncbi.nlm.nih.gov/pubmed/11832223>
- Gabilondo, I., Martínez-Lapiscina, E., Martínez-Heras, E., Fraga-Pumar, E., Llufríu, S., Ortiz, S., ... Villoslada, P. (2014). Trans-synaptic axonal

- degeneration in the visual pathway in multiple sclerosis. *Annals of Neurology*, 75(1), 98–107. <https://doi.org/10.1002/ana.24030>
- Gaillard, R., Naccache, L., Pinel, P., Clémenceau, S., Volle, E., Hasboun, D., ... Cohen, L. (2006). Direct intracranial, fMRI, and lesion evidence for the causal role of left Inferotemporal cortex in Reading. *Neuron*, 50(2), 191–204. <https://doi.org/10.1016/j.neuron.2006.03.031>
- Green, M. F., Glahn, D., Engel, S. A., Nuechterlein, K. H., Sabb, F., Strojwas, M., & Cohen, M. S. (2005). Regional brain activity associated with visual backward masking. *Journal of Cognitive Neuroscience*, 17(1), 13–23. <https://doi.org/10.1162/0898929052880011>
- Green, M. F., Lee, J., Cohen, M. S., Engel, S. A., Korb, A. S., Nuechterlein, K. H., ... Glahn, D. C. (2009). Functional neuroanatomy of visual masking deficits in schizophrenia. *Archives of General Psychiatry*, 66(12), 1295–1303. <https://doi.org/10.1001/archgenpsychiatry.2009.132>
- Has Silemek, A. C., Fischer, L., Pöttgen, J., Penner, I.-K., Engel, A. K., Heesen, C., ... Stellmann, J.-P. (2020). Functional and structural connectivity substrates of cognitive performance in relapsing remitting multiple sclerosis with mild disability. *NeuroImage: Clinical*, 25, 102177. <https://doi.org/10.1016/j.nicl.2020.102177>
- Heesen, C., Haase, R., Melzig, S., Poettgen, J., Berghoff, M., Paul, F., ... Stellmann, J. P. (2018). Perceptions on the value of bodily functions in multiple sclerosis. *Acta Neurologica Scandinavica*, 137(3), 356–362. <https://doi.org/10.1111/ane.12881>
- Horga, G., & Maia, T. V. (2012). Conscious and unconscious processes in cognitive control: A theoretical perspective and a novel empirical approach. *Frontiers in Human Neuroscience*, 6, 199. <https://doi.org/10.3389/fnhum.2012.00199>
- Ito, T., & Yamazaki, K. (2016). A study of a driver model using unconscious driving Behaviors. *Procedia Computer Science*, 96(1), 754–761. <https://doi.org/10.1016/j.procs.2016.08.260>
- Jakimovski, D., Benedict, R. H. B., Weinstock-Guttman, B., Ozel, O., Fuchs, T. A., Lincoff, N., ... Zivadinov, R. (2021). Visual deficits and cognitive assessment of multiple sclerosis: Confounder, correlate, or both? *Journal of Neurology*, 1, 3. <https://doi.org/10.1007/s00415-021-10437-5>
- Julian, L. J. (2011). Cognitive functioning in multiple sclerosis. *Neurologic Clinics*, 29, 507–525. <https://doi.org/10.1016/j.ncl.2010.12.003>
- Kleinschmidt, A., Büchel, C., Hutton, C., Friston, K. J., & Frackowiak, R. S. J. (2002). The neural structures expressing perceptual hysteresis in visual letter recognition. *Neuron*, 34(4), 659–666. <https://doi.org/10.1016/S0896-6273>
- Köhler, W., Fischer, M., Bublak, P., Faiss, J. H., Hoffmann, F., Kunkel, A., ... Penner, I. K. (2017). Information processing deficits as a driving force for memory impairment in MS: A cross-sectional study of memory functions and MRI in early and late stage MS. *Multiple Sclerosis and Related Disorders*, 18, 119–127. <https://doi.org/10.1016/j.msard.2017.09.026>
- Kranczoch, C., Debener, S., Schwarzbach, J., Goebel, R., & Engel, A. K. (2005). Neural correlates of conscious perception in the attentional blink. *NeuroImage*, 24(3), 704–714. <https://doi.org/10.1016/j.neuroimage.2004.09.024>
- Kurtzke, J. F. (1983). Rating neurologic impairment in multiple sclerosis: An expanded disability status scale (EDSS). *Neurology*, 33(11), 1444–1452. Retrieved from. <http://www.ncbi.nlm.nih.gov/pubmed/6685237>
- Lau, H. C., & Passingham, R. E. (2006). Relative blindsight in normal observers and the neural correlate of visual consciousness. *Proceedings of the National Academy of Sciences of the United States of America*, 103(49), 18763–18768. <https://doi.org/10.1073/pnas.0607716103>
- Lau, H. C., & Passingham, R. E. (2007). Unconscious activation of the cognitive control system in the human prefrontal cortex. *Journal of Neuroscience*, 27(21), 5805–5811. <https://doi.org/10.1523/JNEUROSCI.4335-06.2007>
- Lee, J., Cohen, M. S., Engel, S. A., Glahn, D., Nuechterlein, K. H., Wynn, J. K., & Green, M. F. (2014). Neural substrates of visual masking by object substitution in schizophrenia. *Human Brain Mapping*, 35(9), 4654–4662. <https://doi.org/10.1002/hbm.22501>
- Leopold, D. A. (2012). Primary visual cortex: Awareness and Blindsight. *Annual Review of Neuroscience*, 35(1), 91–109. <https://doi.org/10.1146/annurev-neuro-062111-150356>
- Lorscheider, J., Buzzard, K., Jokubaitis, V., Spelman, T., Havrdova, E., Horakova, D., ... Kalincik, T. (2016). Defining secondary progressive multiple sclerosis. *Brain*, 139(9), 2395–2405. <https://doi.org/10.1093/brain/aww173>
- Luppi, A. I., Craig, M. M., Pappas, I., Finoia, P., Williams, G. B., Allanson, J., ... Stamatakis, E. A. (2019). Consciousness-specific dynamic interactions of brain integration and functional diversity. *Nature Communications*, 10(1), 4616. <https://doi.org/10.1038/s41467-019-12658-9>
- Marchetti, G. (2018). Consciousness: A unique way of processing information. *Cognitive Processing*, 19(3), 435–464. <https://doi.org/10.1007/s10339-018-0855-8>
- Markov, N. T., Ercsey-Ravasz, M., Lamy, C., Gomes, A. R. R., Magrou, L., Misery, P., ... Kennedy, H. (2013). The role of long-range connections on the specificity of the macaque interareal cortical network. *Proceedings of the National Academy of Sciences of the United States of America*, 110(13), 5187–5192. <https://doi.org/10.1073/pnas.1218972110>
- Mashour, G. A., Roelfsema, P., Changeux, J.-P., & Dehaene, S. (2020). Conscious processing and the global neuronal workspace hypothesis. *Neuron*, 105(5), 776–798. <https://doi.org/10.1016/j.neuron.2020.01.026>
- McColgan, P., Razi, A., Gregory, S., Seunarine, K. K., Durr, A., Roos, A. C., ... Tabrizi, S. J. (2017). Structural and functional brain network correlates of depressive symptoms in premanifest Huntington's disease. *Human Brain Mapping*, 38(6), 2819–2829. <https://doi.org/10.1002/hbm.23527>
- Meijer, K. A., Steenwijk, M. D., Douw, L., Schoonheim, M. M., & Geurts, J. J. G. (2020). Long-range connections are more severely damaged and relevant for cognition in multiple sclerosis. *Brain*, 143(1), 150–160. <https://doi.org/10.1093/brain/awz355>
- Milner, A. D., & Goodale, M. A. (2008). Two visual systems re-viewed. *Neuropsychologia*, 46(3), 774–785. <https://doi.org/10.1016/j.neuropsychologia.2007.10.005>
- Morin, A. (2017). The “self-awareness–anosognosia” paradox explained: How can one process be associated with activation of, and damage to, opposite sides of the brain? *Laterality: Asymmetries of Body, Brain and Cognition*, 22(1), 105–119. <https://doi.org/10.1080/1357650X.2016.1173049>
- Narain, C. (2005). Object-specific unconscious processing. *Nature Neuroscience*, 8(10), 1288. <https://doi.org/10.1038/nn1005-1288>
- Nguyen, J., Rothman, A., Fitzgerald, K., Whetstone, A., Syc-Mazurek, S., Aquino, J., ... Saida, S. (2018). Visual pathway measures are associated with neuropsychological function in multiple sclerosis. *Current Eye Research*, 43(7), 941–948. <https://doi.org/10.1080/02713683.2018.1459730>
- Nygaard, G. O., De Rodez Benavent, S. A., Harbo, H. F., Laeng, B., Sowa, P., Damangir, S., ... Celiuș, E. G. (2015). Eye and hand motor interactions with the symbol digit modalities test in early multiple sclerosis. *Multiple Sclerosis and Related Disorders*, 4(6), 585–589. <https://doi.org/10.1016/j.msard.2015.08.003>
- Panagiotaropoulos, T. I., Dwarakanath, A., & Kapoor, V. (2020). Prefrontal cortex and consciousness: Beware of the signals. *Trends in Cognitive Sciences*, 24, 343–344. <https://doi.org/10.1016/j.tics.2020.02.005>
- Pessiglione, M., Petrovic, P., Daunizeau, J., Palminteri, S., Dolan, R. J., & Frith, C. D. (2008). Subliminal instrumental conditioning demonstrated in the human brain. *Neuron*, 59(4), 561–567. <https://doi.org/10.1016/j.neuron.2008.07.005>
- Pinto, M. F., Oliveira, H., Batista, S., Cruz, L., Pinto, M., Correia, I., ... Teixeira, C. (2020). Prediction of disease progression and outcomes in multiple sclerosis with machine learning. *Scientific Reports*, 10(1), 1–13. <https://doi.org/10.1038/s41598-020-78212-6>
- Polman, C. H., Reingold, S. C., Banwell, B., Clanet, M., Cohen, J. A., Filippi, M., ... Wolinsky, J. S. (2011). Diagnostic criteria for multiple

- sclerosis: 2010 revisions to the McDonald criteria. *Annals of Neurology*, 69(2), 292–302. <https://doi.org/10.1002/ana.22366>
- Reuter, F., Del Cul, A., Audoin, B., Malikova, I., Naccache, L., Ranjeva, J. P., ... Pelletier, J. (2007). Intact subliminal processing and delayed conscious access in multiple sclerosis. *Neuropsychologia*, 45(12), 2683–2691. <https://doi.org/10.1016/J.NEUROPSYCHOLOGIA.2007.04.010>
- Reuter, F., Del Cul, A., Malikova, I., Naccache, L., Confort-Gouny, S., Cohen, L., ... Audoin, B. (2009). White matter damage impairs access to consciousness in multiple sclerosis. *NeuroImage*, 44(2), 590–599. <https://doi.org/10.1016/j.neuroimage.2008.08.024>
- Rocca, M. A., Vacchi, L., Rodegher, M., Meani, A., Martinelli, V., Possa, F., ... Filippi, M. (2017). Mapping face encoding using functional MRI in multiple sclerosis across disease phenotypes. *Brain Imaging and Behavior*, 11(5), 1238–1247. <https://doi.org/10.1007/s11682-016-9591-9>
- Rossetti, Y., Pisella, L., & McIntosh, R. D. (2017). Rise and fall of the two visual systems theory. *Annals of Physical and Rehabilitation Medicine*, 60, 130–140. <https://doi.org/10.1016/j.rehab.2017.02.002>
- Smith, A. (1982). Symbol digit modality test (SDMT): manual (revised). Los Angeles, CA: Psychological Services.
- Smith, S. M., Jenkinson, M., Johansen-Berg, H., Rueckert, D., Nichols, T. E., Mackay, C. E., ... Behrens, T. E. J. (2006). *Tract-based spatial statistics: Voxelwise analysis of multi-subject diffusion data*, 31, 1487–1505. <https://doi.org/10.1016/j.neuroimage.2006.02.024>
- Soon, C. S., He, A. H., Bode, S., & Haynes, J. D. (2013). Predicting free choices for abstract intentions. *Proceedings of the National Academy of Sciences of the United States of America*, 110(15), 6217–6222. <https://doi.org/10.1073/pnas.1212218110>
- Soto, D., Mäntylä, T., & Silvanto, J. (2011). Working memory without consciousness. *CURBIO*, 21, R912–R913. <https://doi.org/10.1016/j.cub.2011.09.049>
- Stein, T., & Sterzer, P. (2014). Unconscious processing under interocular suppression: Getting the right measure. *Frontiers in Psychology*, 5, 387. <https://doi.org/10.3389/fpsyg.2014.00387>
- Stellmann, J., Young, K., Pöttgen, J., Dorr, M., & Heesen, C. (2015). Introducing a new method to assess vision: Computer-adaptive contrast-sensitivity testing predicts visual functioning better than charts in multiple sclerosis patients. *Multiple Sclerosis Journal - Experimental, Translational and Clinical*, 1, 205521731559618. <https://doi.org/10.1177/2055217315596184>
- Stellmann, J. P., Hodecker, S., Cheng, B., Wanke, N., Young, K. L., Hilgetag, C., ... Siemonsen, S. (2017). Reduced rich-club connectivity is related to disability in primary progressive MS. *Neurology: Neuroimmunology and Neuroinflammation*, 4(5), 1–10. <https://doi.org/10.1212/NXI.0000000000000375>
- Sterzer, P., Haynes, J. D., & Rees, G. (2008). Fine-scale activity patterns in high-level visual areas encode the category of invisible objects. *Journal of Vision*, 8(15), 10.1–10.1012. <https://doi.org/10.1167/8.15.10>
- Sumowski, J. F., Benedict, R., Enzinger, C., Filippi, M., Geurts, J. J., Hamalainen, P., ... Rao, S. (2018). Cognition in multiple sclerosis: State of the field and priorities for the future. *Neurology*, 90(6), 278–288. <https://doi.org/10.1212/WNL.0000000000004977>
- Tononi, G., Boly, M., Massimini, M., & Koch, C. (2016). Integrated information theory: From consciousness to its physical substrate. *Nature Reviews Neuroscience*, 17, 450–461. <https://doi.org/10.1038/nrn.2016.44>
- Tournier, J.-D., Smith, R., Raffelt, D., Tabbara, R., Dhollander, T., Pietsch, M., ... Connelly, A. (2019). MRtrix3: A fast, flexible and open software framework for medical image processing and visualisation. *NeuroImage*, 202, 116137. <https://doi.org/10.1016/J.NEUROIMAGE.2019.116137>
- van Gaal, S., de Lange, F. P., & Cohen, M. X. (2012). The role of consciousness in cognitive control and decision making. *Frontiers in Human Neuroscience*, 6, 121. <https://doi.org/10.3389/fnhum.2012.00121>
- Van Gaal, S., & Lamme, V. A. F. (2012). Unconscious high-level information processing: Implication for neurobiological theories of consciousness. *The Neuroscientist*, 18(3), 287–301. <https://doi.org/10.1177/1073858411404079>
- Van Gaal, S., Ridderinkhof, K. R., Scholte, H. S., & Lamme, V. A. F. (2010). Unconscious activation of the prefrontal no-go network. *Journal of Neuroscience*, 30(11), 4143–4150. <https://doi.org/10.1523/JNEUROSCI.2992-09.2010>
- van Geest, Q., Douw, L., van't Klooster, S., Leurs, C. E., Genova, H. M., Wylie, G. R., ... Hulst, H. E. (2018). Information processing speed in multiple sclerosis: Relevance of default mode network dynamics. *NeuroImage: Clinical*, 19, 507–515. <https://doi.org/10.1016/j.nicl.2018.05.015>
- van Geest, Q., Hulst, H. E., Meijer, K. A., Hoyng, L., Geurts, J. J. G., & Douw, L. (2018). The importance of hippocampal dynamic connectivity in explaining memory function in multiple sclerosis. *Brain and Behavior: A Cognitive Neuroscience Perspective*, 8(5), e00954. <https://doi.org/10.1002/brb3.954>
- Veréb, D., Tóth, E., Bozsik, B., Király, A., Szabó, N., Kincses, B., ... Kincses, Z. T. (2020). Altered brain network function during attention-modulated visual processing in multiple sclerosis. *Multiple Sclerosis Journal*. <http://dx.doi.org/10.1177/1352458520958360>
- Volz, L. J., & Gazzaniga, M. S. (2017). Interaction in isolation: 50 years of insights from split-brain research. *Brain*, 140(7), 2051–2060. <https://doi.org/10.1093/brain/awx139>
- Watanabe, M., Cheng, K., Murayama, Y., Ueno, K., Asamizuya, T., Tanaka, K., & Logothetis, N. (2011). Attention but not awareness modulates the BOLD signal in the human V1 during binocular suppression. *Science*, 334(6057), 829–831. <https://doi.org/10.1126/science.1203161>
- Wieder, L., Gäde, G., Pech, L. M., Zimmermann, H., Wernecke, K. D., Dörr, J. M., ... Brandt, A. U. (2013). Low contrast visual acuity testing is associated with cognitive performance in multiple sclerosis: A cross-sectional pilot study. *BMC Neurology*, 13(1), 167. <https://doi.org/10.1186/1471-2377-13-167>
- Zalesky, A., Fornito, A., & Bullmore, E. T. (2010). Network-based statistic: Identifying differences in brain networks. *NeuroImage*, 53(4), 1197–1207. <https://doi.org/10.1016/j.neuroimage.2010.06.041>

SUPPORTING INFORMATION

Additional supporting information may be found online in the Supporting Information section at the end of this article.

How to cite this article: Has Silemek AC, Ranjeva J-P, Audoin B, et al. Delayed access to conscious processing in multiple sclerosis: Reduced cortical activation and impaired structural connectivity. *Hum Brain Mapp*. 2021;1–17. <https://doi.org/10.1002/hbm.25440>